

“© 2021 IEEE. Personal use of this material is permitted. Permission from IEEE must be obtained for all other uses, in any current or future media, including reprinting/republishing this material for advertising or promotional purposes, creating new collective works, for resale or redistribution to servers or lists, or reuse of any copyrighted component of this work in other works.”

Frequency Domain Pilot-Aided Channel Estimation for OTFS over Fast Fading Channels

Hongyang Zhang, Xiaojing Huang, and J. Andrew Zhang

University of Technology Sydney, Ultimo, NSW, 2007, Australia

Emails: Hongyang.ZHANG-1@student.uts.edu.au

{Xiaojing.Huang, Andrew.Zhang}@uts.edu.au

Abstract—Achieving better performance in high mobility scenarios has become an emerging topic for next generation wireless communications. Compared with traditional modulation techniques, the recently proposed orthogonal time frequency space (OTFS) shows outstanding performance over fast fading channels. In this paper, the OTFS system is first represented in the form of precoded orthogonal frequency division multiplexing (OFDM), enabling traditional estimation and equalization techniques to work under fast fading channels. Then, a novel frequency-domain pilot-aided channel estimation scheme is proposed to obtain the channel state information at the receiver. Simulation results show that the new channel estimation scheme works efficiently in different channel scenarios. Meanwhile, the overhead of the proposed scheme is also lower than those of the current popular schemes.

Index Terms—Precoded OFDM, OTFS, channel estimation, fast fading channel

I. INTRODUCTION

NEXT generation network requires reliable, high capacity and low-latency communication in high mobility scenarios, such as vehicles to everything networks (V2X) and unmanned aerial vehicle networks (UAV). As the current popular modulation, orthogonal frequency division multiplexing (OFDM), has difficulty in coping with fast fading channels, the development of new techniques is of high priority.

In recent years, orthogonal time frequency space (OTFS) modulation has shown outstanding performance in fast fading channels compared with other traditional modulations [1]. Different from traditional methods, the signal of OTFS is modulated in the delay-Doppler domain through inverse symplectic finite Fourier transform (ISFFT). It has the capability of exploiting both time and frequency diversity.

An accurate channel estimation (CE) is significant for recovering the transmitted data information. Existing CE techniques for OTFS are mostly based on delay-Doppler domain pilot-adding method. An embedded pilot-added channel estimation scheme is proposed in [2], where a pilot in the delay-Doppler domain is inserted and surrounded by suitable zero guard intervals (GI). However, it introduces the peak to average power ratio (PAPR) problem and has high computational complexity. A corner-inserted pilot pattern (CIPP) is proposed in [3] to ease these problems. Based on different pilot patterns, maximum likelihood (ML) [4], sparse Bayesian learning algorithm [5], and linear minimum mean square error (LMMSE)

[3] are employed to achieve the balance between performance and complexity. Moreover, delay-Doppler domain pilot-adding method is also extended to multiple-input multiple-output (MIMO) OTFS systems. A delay-Doppler-angle three-dimensional orthogonal matching pursuit (3D-OMP) algorithm is proposed in [6] to achieve a sparse channel. Different pilot patterns, such as [7], are employed to avoid overlapping issues and improve the performance.

In this paper, we first review fast fading channel models and obtain the relationships among different domains. We highlight that the frequency-Doppler domain channel matrix has a concise stripe diagonal structure. We then prove that OTFS can be represented as a more general precoded OFDM system, and this transformation converts signals from the delay-Doppler domain to the frequency domain. Based on this channel expression, a novel frequency-domain pilot scheme is proposed to achieve accurate channel state information (CSI). The main contributions of this paper are summarized as follows.

- First, the OTFS is formulated as a precoded-OFDM, enabling OTFS to adopt well-established techniques for channel estimation and equalization to cope with fast fading channels.
- Second, frequency-domain pilot and estimation are proposed, achieving both low-complexity and high performance. Meanwhile, the pilot overhead and the PAPR can also be controlled.

The rest of the paper is organized as follows. In Section II, the fast fading channel representation in the frequency-Doppler domain is developed and the OTFS modulation is formulated as a precoded OFDM system. In Section III, the frequency-domain pilot insertion and channel estimation are proposed for both integer and fractional Doppler cases. Simulation results are provided in Section IV to compare the performance under different channel conditions. Finally, conclusions are drawn in Section V.

II. CHANNEL AND SYSTEM MODELS

In this section, channel representations in different domains over fast fading channels are first developed. The OTFS system is then reviewed and expressed as a precoded OFDM system, enabling the application of frequency-domain channel

estimation methods to obtain CSI at the receiver. In this paper, only single-input-single-output (SISO) system is considered.

A. Fast Fading Channel Models

In high mobility systems, the interferences mainly come from delays and Doppler frequency shifts in the multipath. Assuming that a signal sequence is transmitted through the fast fading channel, the received signal in the continuous-time domain can be expressed as

$$r(t) = \int_{-\infty}^{+\infty} \int_{-\infty}^{+\infty} h(\tau, \nu) s(t - \tau) e^{j2\pi\nu t} d\tau d\nu + w(t), \quad (1)$$

where $s(t)$ is the time-domain transmitted signal, $h(\tau, \nu)$ is the *delay-Doppler spreading function* of the fast fading channel, $\mathbf{j} = \sqrt{-1}$ and $w(t)$ is the additive white Gaussian noise (AWGN). For a sparse P -path channel, $h(\tau, \nu)$ is defined as

$$h(\tau, \nu) = \sum_{i=1}^P h_i \delta(\tau - \tau_i) \delta(\nu - \nu_i), \quad (2)$$

where h_i , τ_i , and ν_i are the path gain, delay and Doppler shift of the i -th path, respectively, and $\delta(\cdot)$ denotes the Dirac delta function.

Based on the delay-Doppler channel model, representations of the fast fading channel in other domains can be obtained through Fourier transform (FT) and inverse Fourier transform (IFT). Specific relationships can be found in [8].

In this paper, we concentrate on the frequency-domain estimation scheme development. Applying FT to $h(\tau, \nu)$ with respect to delay τ , the *frequency-Doppler* representation can be expressed as

$$H_\nu(f, \nu) = \int_{-\infty}^{+\infty} h(\tau, \nu) e^{-j2\pi f \tau} d\tau. \quad (3)$$

Then, the continuous-time domain expression will be transformed to frequency domain in the following analysis. Denotations in the time domain are complemented as follows. The transmitted signal can be expressed as $s[i] = s(id_r)$, $i = 0, 1, \dots, MN - 1$, where d_r is the *delay resolution* or the sampling period. Assuming that the maximum delay in the multipath channel is d_{max} , the maximum number of resolvable multipaths can be expressed as $L_{max} = \lceil d_{max}/d_r \rceil$, where $\lceil \cdot \rceil$ denotes the ceiling function to obtain the rounded up number, with the required minimum channel bandwidth of $1/d_r$. Denoting f_r as the *Doppler resolution* and f_{max} as the maximum Doppler frequency shift, the maximum number of positive resolvable Doppler frequencies can be expressed as $K_{max} = \lceil f_{max}/f_r \rceil$ over a minimum frame length of $1/f_r$ for the transmitted signals. Note that there are both positive and negative Doppler frequency shifts in the fast fading channel, which means that the Doppler resolution range is $[-K_{max}, K_{max}]$.

Based on Eq. (3) and applying FT to $r(t)$ in (1), the frequency-domain received signal can be modeled as

$$\begin{aligned} R(f) &= \int_{-\infty}^{+\infty} r(t) e^{-j2\pi f t} dt + W(f) \\ &= \int_{-\infty}^{+\infty} \int_{-\infty}^{+\infty} H(f', t) e^{-j2\pi(f-f')t} dt S(f') df' + W(f) \\ &= \int_{-\infty}^{+\infty} H_\nu(f', f - f') S(f') df' + W(f), \end{aligned} \quad (4)$$

where $S(f)$ is the FT of $s(t)$ and $W(f)$ is the AWGN in the frequency domain.

From (3), the discrete frequency-Doppler domain channel representation can be expressed as

$$H_\nu[i, j] = H_\nu(i f_\Delta, \bar{\nu}_j) = \int H(i \Delta f, t) e^{-j2\pi \bar{\nu}_j t} dt, \quad (5)$$

Here, f_Δ denotes the subcarrier frequency spacing and $\bar{\nu}_j$ is the j -th quantized Doppler frequency. Denoting the transmitted and received signal sequences in the discrete-frequency domain as \mathbf{S} and \mathbf{R} respectively, the discrete-frequency domain received signal can be expressed from (4) in matrix form as

$$\mathbf{R} = \mathbf{H}_\nu \mathbf{S} + \mathbf{W}, \quad (6)$$

where \mathbf{W} denotes the frequency-domain noise vector and \mathbf{H}_ν is the frequency-Doppler domain channel matrix expressed as

$$\mathbf{H}_\nu = \begin{bmatrix} H_\nu[0, 0] & \cdots & H_\nu[MN - 1, 1] \\ H_\nu[0, 1] & \cdots & H_\nu[MN - 1, 2] \\ \vdots & \ddots & \vdots \\ H_\nu[0, MN - 1] & \cdots & H_\nu[MN - 1, 0] \end{bmatrix}. \quad (7)$$

Through (2) and (5), $H_\nu[i, j]$ can be obtained given arbitrary h_i , τ_i and ν_i in any sparse P -path channel.

Fig. 1 shows the construction of (7), in which the shaded squares show the non-zero elements in the matrix, whereas the blank squares show the zero elements. Note that, due to the discretization of $H_\nu(f', \nu)$ as shown in (5), $H_\nu[i, j]$ is periodical in the Doppler domain represented by the index j . When the Doppler frequency shift ν is confined in $[-K_{max}, K_{max}]$, after the coordination transform $\nu = f - f'$, the Doppler shift values appear in the diagonal stripe of width $2K_{max} + 1$ on the f - f' plane. We observe that the frequency-Doppler domain channel matrix demonstrates a stripe diagonal structure with stripe width $2K_{max} + 1$. As we illustrated in [8], the stripe-diagonal structure of frequency-domain channel matrix \mathbf{H}_ν can reduce the receiver signal processing complexity significantly, and also works well for off-grid path delays and Doppler shifts. Therefore, our estimation technique is based on the frequency domain channel model and also capable of dealing with both integer and fractional Doppler conditions, which will be further demonstrated in Section III.

B. OTFS as Precoded OFDM

In the original OTFS system, the data symbols after constellation mapping are arranged in a two dimensional (2D) $M \times N$ matrix \mathbf{X} , where M denotes the number of elements

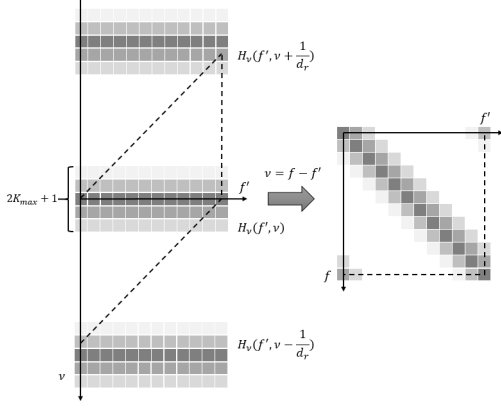


Fig. 1. Construction of channel matrix \mathbf{H}_ν from $H_\nu[i, j]$.

in delay dimension, N denotes the number of elements in Doppler dimension, and $\mathbf{X} \in \mathbb{C}^{M \times N}$. In the vector form, the data symbols to be transmitted can be expressed as $\mathbf{x} = \text{vec}(\mathbf{X})$ where $\text{vec}(\cdot)$ is the vectorizing function. After ISFFT, Heisenberg transform and the pulse shaping, the time-domain signal is transmitted through the fast fading channel. Assuming the pulse shaping operation is a rectangular window function, the signal matrix to be sent into the channel can be expressed as

$$\mathbf{D} = \mathbf{F}_M^H (\mathbf{F}_M \mathbf{X} \mathbf{F}_N^H) = \mathbf{X} \mathbf{F}_N^H, \quad (8)$$

where \mathbf{D} is an $M \times N$ matrix, \mathbf{F}_N denotes the N -point FFT matrix. The time-domain signal to be transmitted is the vectorized data matrix \mathbf{D} expressed as

$$\mathbf{s} = \text{vec}(\mathbf{D}) = (\mathbf{F}_N^H \otimes \mathbf{I}_M) \mathbf{x}, \quad (9)$$

where \mathbf{s} is an $MN \times 1$ vector, \otimes denotes Kronecker product. From (6) and (9), the received frequency-domain signal can be expressed as

$$\mathbf{R} = \mathbf{H}_\nu \mathbf{F}_{MN} (\mathbf{F}_N^H \otimes \mathbf{I}_M) \mathbf{x} + \mathbf{W}. \quad (10)$$

According to the Cooley-Tukey general factorization, the MN -point discrete Fourier transform (DFT) \mathbf{F}_{MN} can be factorized as two smaller DFTs in terms of sizes M and N , which can be expressed as

$$\mathbf{F}_{MN} = \mathbf{P}_{M,N} (\mathbf{I}_N \otimes \mathbf{F}_M) \text{diag}(e^{-j \frac{2\pi}{MN} (i)_M \lfloor \frac{i}{M} \rfloor}) (\mathbf{F}_N \otimes \mathbf{I}_M), \quad (11)$$

where $\text{diag}(x_i)$, $i = 0, \dots, MN - 1$, denotes a diagonal matrix with the i -th diagonal element x_i , $(\cdot)_M$ denotes modulo M operation, $\lfloor \cdot \rfloor$ denotes flooring operation and $\mathbf{P}_{M,N}$ denotes a permutation matrix of dimension $MN \times MN$. The permutation matrix equivalently performs the interleaving operation that reads the elements in the matrix column-wise and stacks them to a matrix row-wise.

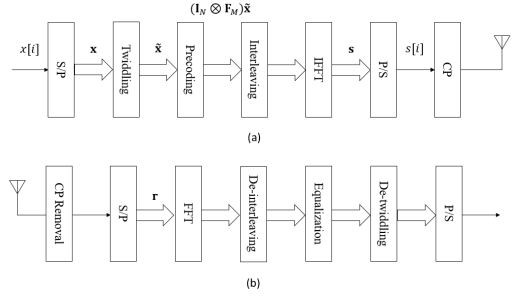


Fig. 2. OTFS system block diagram in precoded OFDM form: (a) transmitter and (b) receiver. S/P and P/S stand for serial-to-parallel and parallel-to-serial conversions respectively, and CP stands for cyclic prefix.

Therefore, based on (10) and (11), the received frequency-domain signal becomes

$$\mathbf{R} = \mathbf{H}_\nu \mathbf{P}_{M,N} (\mathbf{I}_N \otimes \mathbf{F}_M) \text{diag}(e^{-j \frac{2\pi}{MN} (i)_M \lfloor \frac{i}{M} \rfloor}) \mathbf{x} + \mathbf{W} \quad (12)$$

and the OTFS system can be transformed into a precoded OFDM system as illustrated in Fig. 2, where $(\mathbf{I}_N \otimes \mathbf{F}_M)$ is the precoding matrix, which is also an unitary matrix, and $\tilde{\mathbf{x}} = \text{diag}(e^{-j \frac{2\pi}{MN} (i)_M \lfloor \frac{i}{M} \rfloor}) \mathbf{x}$ is the twiddled signal vector. Note that the twiddling will only affect the phase of the symbol, and will not affect the signal detection and the bit error rate (BER) performance after de-twiddling at the receiver. Excluding the twiddling at the transmitter and the de-twiddling at the receiver, Fig. 2 shows a typical precoded OFDM system. Based on the above transmission, the previous 2D OTFS system in the delay-Doppler domain is expressed as a 1D precoded OFDM system in the frequency domain. Therefore, corresponding frequency-domain pilots can be designed for channel estimation according to the channel matrix shown in (7). At the receiver, frequency domain equalizations, such as MMSE [8], can also be applied to recover the signals.

III. CHANNEL ESTIMATION

A. Pilot-Adding Schemes for Integer Doppler Case

Exploiting the simple stripe-diagonal structure of the frequency-domain channel matrix, comb-type pilots are proposed in our systems and we assume that pilots are added in each OTFS symbol. According to Fig. 2, the initial data vector to be transmitted can be expressed as \mathbf{x} . After twiddling, precoding and interleaving, the signal is ready to be transformed into the time domain. Note that our pilot-adding process is completed before IFFT. Fig. 3 shows the method of pilot-adding, where shaded patterns denote non-zero elements and blank circles denote zeros. Precoded symbols are reshaped into an M' by N' matrix after interleaving, where N' is set not less than L_{max} to ensure that estimation can fully explore time-domain diversity. $2K_{max}$ guard intervals are added on both sides of each pilot respectively to prevent the frequency-domain channel information from being interfered by data symbols. After the pilot adding, the symbols are reshaped to an $N'(M' + 4K_{max} + 1)$ by 1 vector and transformed into the time

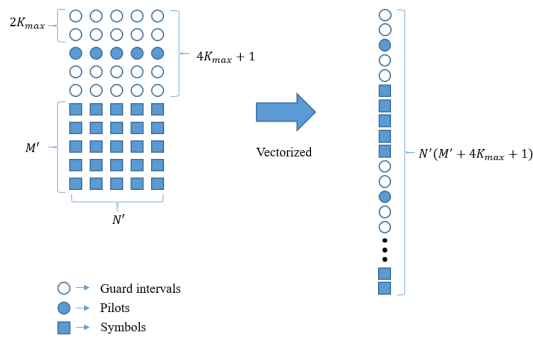


Fig. 3. The structure of frequency-domain pilots.

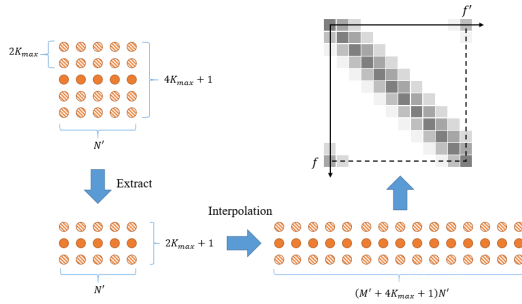


Fig. 4. Structure of estimator.

domain through IFFT of the size $N'(M' + 4K_{max} + 1)$. Overall, the overhead of frequency-domain pilot is $L(4K_{max} + 1)$, which is much less than the $(2L + 1)(4K_{max} + 1)$ (integer Doppler cases) and $(2L + 1)N'$ (fractional Doppler cases) in the popular delay-Doppler domain embedded channel estimation [2].

Fig. 4 shows the process of channel estimation. At the receiver, the received signals are transformed into frequency domain first and then pilots are extracted. Here we still reshape them into a $4K_{max} + 1$ by N' matrix for better illustration. Since the stripe width of the frequency-domain channel matrix is $2K_{max} + 1$, only the central $2K_{max} + 1$ frequency bins carry channel state information, and the other $2K_{max}$ frequency bins on both sides are contaminated by transmitted symbols. Therefore, the central $2K_{max}$ frequency bins are extracted and then interpolated, and finally an estimated channel can be reconstructed. The detailed processing will be mathematical illustrated in Section III.C.

B. Pilot-Adding Schemes for Fractional Doppler Case

Many channel estimation techniques based on delay-Doppler domain pilots divide Doppler frequencies into integer and fractional conditions because they produce different channel responses in this 2D domain and different pilot-guard patterns are needed [2]. However, for our frequency-domain estimation scheme, the integer Doppler pilot pattern can also work in fractional Doppler cases. As we know, the channel matrix represents a discrete sampling of the channel, no matter

whether it is an accurate or estimated one. Meanwhile, the integer and fractional Doppler cases can also be regarded as the Doppler shifts on and off the grid respectively. However, for both conditions, the discrete channel representation can be obtained from (5). Therefore, even for the fractional Doppler case, its characteristics can be reflected by the discrete channel matrix.

C. Channel Estimation and Performance Analysis

Assume a pilot vector with guard intervals is extracted from pilot-added signal. It can be expressed as $\mathbf{s}_p = [\mathbf{s}_{p1}, \mathbf{s}_{p2}, \dots, \mathbf{s}_{pN'}]$ in the frequency domain, where

$$\mathbf{s}_{p1} = \dots = \mathbf{s}_{pN'} = \underbrace{[0, 0, \dots, 0]}_{2k}, V_p, \underbrace{[0, 0, \dots, 0]}_{2k}^T, \quad (13)$$

and V_p indicates the value of pilot. According to Fig. 4, the received useful pilot bins are $N'(2K_{max} + 1)$ in total and can be expressed as

$$\begin{aligned} \mathbf{R}_P &= \mathbf{R}((M' + 4K_{max} + 1)n + k) \\ &= \mathbf{H}_V((M' + 4K_{max} + 1)n + 2K_{max}, \\ & (M' + 4K_{max} + 1)n + k)V_p + \mathbf{W}((M' + 4K_{max} + 1)n + k) \\ &= \mathbf{H}_P V_p + \mathbf{W}_P, \end{aligned} \quad (14)$$

where $n = 0, \dots, N' - 1, k = K_{max}, \dots, 3K_{max}$ and \mathbf{P} is a $N'(2K_{max} + 1)$ by $N'(2K_{max} + 1)$ diagonal matrix with all diagonal elements equaling V_p .

Note that the received useful pilot \mathbf{R}_P reflects a sampling at evenly spaced N' frequency bins from $N'(M' + 4K_{max} + 1)$ by $N'(M' + 4K_{max} + 1)$ channel matrix. Therefore, \mathbf{R}_P can be reshaped to an $(2K_{max} + 1)$ by N' matrix, where the $(2K_{max} + 1)$ dimension indicates the Doppler and the N' dimension indicates the frequency. Then, the estimation of the channel $\hat{\mathbf{H}}_P$ can be obtained by dividing \mathbf{R}_P by the pilot value V_p . Interpolating estimation result with respect to frequency dimension, a complete $N'(M' + 4K_{max} + 1)$ by $(2K_{max} + 1)$ estimation of the whole channel matrix can be obtained and finally the channel matrix can be constructed as shown in Fig. 4. Also note that the equivalent subcarriers is very small as MN is very large so that the correlations between $\mathbf{H}_V(n, m)$ along the subcarriers n are very high.

From Eq. (14), an estimate of pilot channel matrix can be expressed as

$$\hat{\mathbf{H}}_P = \mathbf{R}_P \mathbf{P}^{-1} = \mathbf{H}_P + \mathbf{W}_P \mathbf{P}^{-1}. \quad (15)$$

Therefore, the MSE of the estimation can be expressed as

$$\begin{aligned} \text{MSE} &= E\{\text{tr}\{(\hat{\mathbf{H}}_P - \mathbf{H}_P)(\hat{\mathbf{H}}_P - \mathbf{H}_P)^H\}\} \\ &= \text{tr}\{(\mathbf{P}^H \mathbf{P})^{-1}\} \sigma_{\mathbf{W}_P}^2. \end{aligned} \quad (16)$$

IV. SIMULATION

In this section, simulations are performed to show the performance of frequency-domain pilots and channel estimation for uncoded OTFS systems. ETSI's tapped delay line (TDL) channel models are adopted [9]. In these models, the time delays and channel gains in all multipath taps are defined

TABLE I
SIMULATION PARAMETERS

Carrier Frequency (f_c)	No. of Subcarriers (M)	No. of OFDM Symbols (N)
6 GHz	256	32
Subcarrier Spacing (f_Δ)	Bandwidth ($W = Mf_\Delta$)	Duration of OFDM/SC-FDMA Symbol ($T = M/W$)
30 KHz	7.68 MHz	33.33 μ s
Delay Resolution ($d_r = 1/W$)	Doppler Resolution ($f_r = 1/NT$)	Maximum Speed (v_{max})
130.21 ns	937.5 Hz	500 Km/h
Maximum Doppler Frequency ($f_{max} = f_c \frac{v_{max}}{v_c}$, $v_c = 3 \times 10^8$ m/s)	No. of Doppler Shifts (Positive or Negative) ($K_{max} = \lceil \frac{f_{max}}{f_r} \rceil$)	No. of Multipaths ($L_{max} = \lceil \frac{d_{max}}{d_r} \rceil$)
2777.8 Hz	≈ 3	≈ 32 (LOS)

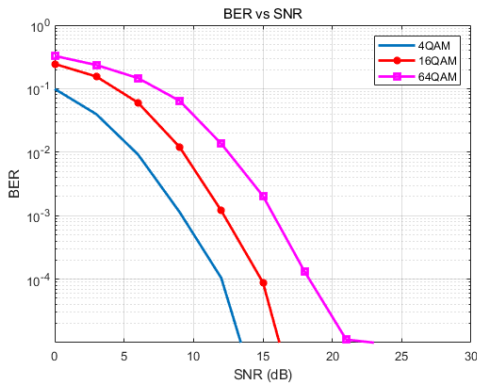


Fig. 5. BER performance under frequency-domain pilot-aided channel estimation with 4, 16 and 64 QAM modulations.

in line-of-sight (LOS) conditions, and the Doppler frequency shifts are uniformly distributed from $-K_{max}$ to K_{max} . In this paper, frequency-domain MMSE equalization is adopted to recover the signal. All the parameters are listed in Table I, in which d_{max} indicates the maximum delay time [9].

Based on the above settings, the overhead of frequency-domain pilots is 5%, while the embedded delay-Doppler-domain pilots have 10% overhead. Fig. 5 shows the BER performance under 4, 16 and 64 quadrature amplitude modulation (QAM). The frequency-domain pilots can effectively perform channel estimation over the fast fading channels.

Furthermore, the BER performance under different maximum speeds is shown in Fig. 6. With the same system parameter settings, as the maximum speed in the channel increases, the BER performance improves slightly. It shows that if the pilot and guard intervals are set properly, the channel information can be obtained with high accuracy and the BER performance is similar to that with perfect channel knowledge. The slight degradation at a low speed is due to the fixed Doppler resolution. Therefore, higher speed enables the

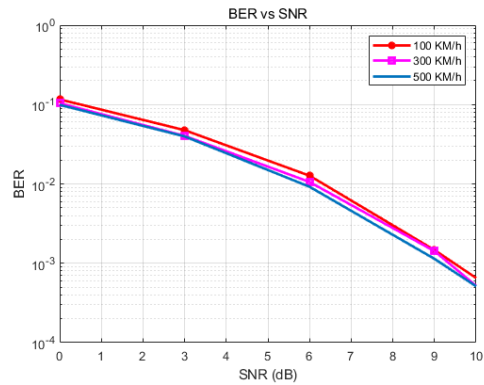


Fig. 6. BER performance under different maximum speed.

exploration of more diversity and the performance is better.

V. CONCLUSION

In this paper, we first revisited the relationships of signals among different domains over fast fading channels. Then, the OTFS system was expressed as precoded OFDM, enabling well-established techniques in traditional modulations to be applied to OTFS systems. Based on the frequency-Doppler channel response, a novel frequency-domain pilot-aided channel estimation scheme was proposed. Compared with current popular delay-Doppler domain pilot and estimation, our method has a much smaller overhead and can efficiently work with frequency domain equalization to recover the transmitted signal.

REFERENCES

- [1] R. Hadani, S. Rakib, M. Tsatsanis, A. Monk, A. J. Goldsmith, A. F. Molisch, and R. Calderbank, "Orthogonal time frequency space modulation," in *2017 IEEE Wireless Communications and Networking Conference (WCNC)*, March 2017, pp. 1–6.
- [2] P. Raviteja, K. T. Phan, and Y. Hong, "Embedded pilot-aided channel estimation for OTFS in delay-doppler channels," *IEEE Transactions on Vehicular Technology*, vol. 68, no. 5, pp. 4906–4917, 2019.
- [3] H. Qu, G. Liu, L. Zhang, M. A. Imran, and S. Wen, "Low-dimensional subspace estimation of continuous-doppler-spread channel in otfs systems," *IEEE Transactions on Communications*, pp. 1–1, 2021.
- [4] L. Gaudio, M. Kobayashi, G. Caire, and G. Colavolpe, "On the effectiveness of otfs for joint radar parameter estimation and communication," *IEEE Transactions on Wireless Communications*, vol. 19, no. 9, pp. 5951–5965, 2020.
- [5] L. Zhao, W.-J. Gao, and W. Guo, "Sparse bayesian learning of delay-doppler channel for otfs system," *IEEE Communications Letters*, vol. 24, no. 12, pp. 2766–2769, 2020.
- [6] W. Shen, L. Dai, J. An, P. Fan, and R. W. Heath, "Channel estimation for orthogonal time frequency space (OTFS) massive MIMO," *IEEE Transactions on Signal Processing*, vol. 67, no. 16, pp. 4204–4217, 2019.
- [7] M. Kollengode Ramachandran and A. Chockalingam, "MIMO-OTFS in high-doppler fading channels: Signal detection and channel estimation," in *2018 IEEE Global Communications Conference (GLOBECOM)*, 2018, pp. 206–212.
- [8] H. Zhang, X. Huang, and J. A. Zhang, "Adaptive transmission with frequency-domain precoding and linear equalization over fast fading channels," *IEEE Transactions on Wireless Communications*, pp. 1–1, 2021.
- [9] ETSI, "Study on channel model for frequencies from 0.5 to 100 GHz," *ETSI TR 138 901 V15.0.0*, July 2018.